Enhanced dissolution and stability of Tanshinone IIA base by solid dispersion system with nano-hydroxyapatite

Yan-rong Jiang[1,2], Zhen-hai Zhang[1], Sai-yan Huang[1], Yan Lu[2], Tian-tian Ma[2], Xiao-bin Jia[1]

[1]Chinese Herb Preparation Room, Key Laboratory of New Drug Delivery System of Chinese Materia Medica, Jiangsu Provincial Academy of Chinese Medicine, Nanjing, Jiangsu, [2]College of Pharmacy, Nanjing University of Chinese Medicine, Nanjing, China

Submitted: 31-12-2012 Revised: 19-01-2013 Published: 24-07-2014

ABSTRACT

Background: Tanshinone IIA (TSIIA) exhibits a variety of cardiovascular effects; however, it has low solubility in water. The preparation of poorly soluble drugs for oral delivery is one of the greatest challenges in the field of formulation research. Among the approaches available, solid dispersion (SD) technique has proven to be one of the most commonly used these methods for improving dissolution and bioavailability of drugs, because of its relative simplicity and economy in terms of both preparation and evaluation. **Objective:** This study was aimed at investigating the dissolution behavior and physical stability of SDs of TSIIA by employing nano-hydroxyapatite (n-HAp). **Materials and Methods:** The TSIIA SDs was prepared to use a spray-drying method. First, an *in vitro* dissolution test was performed to assess dissolution characteristics. Next, a set of complementary techniques (differential scanning calorimetry, scanning electron microscopy, X-ray powder diffraction, and Fourier transform infrared spectroscopy) was used to monitor the physicochemical properties of the SDs. The SDs was stored at 40°C/75% relative humidity for 6 months, after which their stability was assessed. **Results:** TSIIA dissolution remarkably improved because of the formulation of the SDs with n-HAp particles. Comparisons with the corresponding physical mixtures revealed changes in the SDs and explained the formation of the amorphous phase. In the stability test, virtually no time-dependent decrease was observed in either *in vitro* drug dissolution or drug content. **Conclusion:** SD formulation with n-HAp may be a promising approach for enhancing the dissolution and stability of TSIIA.

Key words: Dissolution, nano-hydroxyapatite, solid dispersion, stability, Tanshinone IIA

Access this article online

Website: www.phcog.com

DOI: 10.4103/0973-1296.137375

Quick Response Code:

INTRODUCTION

The number of poorly soluble drug compounds has increased sharply since high-throughput screening and combinatorial chemistry were introduced into pharmaceutical development processes.[1-3] Enhancing the oral bioavailability of poorly water-soluble drugs by an increasing dissolution is one of the most challenging tasks in drug development.[4,5] The various methods such as salt formation, solubilization, particle-size reduction, and solid dispersion (SD) formation have been reported for this purpose.[6-9] Among these, SD technique is frequently used.

Address for correspondence:
Dr. Xiaobin Jia, Key Laboratory of New Drug Delivery System of Chinese Materia Medica, Jiangsu Provincial Academy of Chinese Medicine, 100 Shizi Road, Nanjing, Jiangsu 210028, People's Republic of China.
E-mail: xiaobinjia_nj@126.com

The SD technique is defined as the dispersion of one or more active ingredients within an inert carrier or matrix.[10,11] Although, the SD approach has generated considerable interest, its commercial application has been limited because of difficulties involved in the manufacturing process, as well as problems with product stability.[12,13] Poor stability can result in the reversal of the amorphous drug into a crystalline state and can thus, alter its dissolution properties upon storage. Nevertheless, specific interactions between drugs and their carriers have been reported to inhibit recrystallization and/or stabilize the active ingredient in the amorphous state.[14,15]

Hydroxyapatite ($Ca_{10}(PO_4)_6(OH)_2$), a substantial inorganic component of mammalian bones and teeth, is an excellent biomaterial because of its biocompatibility and osteoconductivity.[16,17] In addition, hydroxyapatite has been used as an adsorbent for a wide range of ions, small molecules, and macromolecules.[18,19] Nano-hydroxyapatite (n-HAp)

exhibits a significant adsorption capacity owing to its relatively large surface area[20] and was found to be a superior sorbent because of its low cost, availability, and high defluoridation capacity, as previously reported by Sairam Sundaram *et al*.[21] n-HAp has also received significant attention for application in medicine and dentistry.[22-24] However, there are currently no reports on the application of n-HAp as a carrier in SD formulations.

Tanshinone IIA (TSIIA), a main biologically active component extracted from the root of *Salvia miltiorrhiza* Bunge, exhibits a variety of cardiovascular effects. It is used to treat cardiovascular and cerebrovascular diseases such as angina pectoris, arrhythmias, acute ischemic stroke, and hyperlipidemia.[25-28] However, TSIIA has low oral bioavailability[29] because of its negligible solubility in water,[30] insufficient dissolution rate,[31,32] and first-pass metabolism.[33]

In the present study, solid dispersions (SDs) was prepared to use the TSIIA and n-Hap, which were used as models of a poorly water-soluble drug and a dispersion carrier, respectively. Physical changes in the SDs were examined using the differential scanning calorimetry (DSC), scanning electron microscopy (SEM), X-ray powder diffraction (XRPD), and Fourier transform infrared spectroscopy (FTIR), and the dissolution performance was evaluated. The stability of the SDs after long-term storage was also tested.

MATERIALS AND METHODS

Materials

A TSIIA standard with purity greater than 99% was purchased from the National Institute for the Control of Pharmaceutical and Biological Products (Beijing, China). In additional TSIIA was supplied by Nanjing ZeLang Medical Technology Co. Ltd., and its purity was greater than 98%; n-HAp with an average particle size of 60 nm was supplied by Nanjing Aipurui Nano Materials Co. Ltd (Nanjing, China). All reagents were of analytical grade except for methanol, which was of chromatographic grade.

Preparation of SDs and physical mixtures

The SDs of TSIIA with n-HAp in the following ratios was prepared to use a spray-drying method: TSIIA: n-Hap at ratios of 1:2, 1:4, 1:6, and 1:8. TSIIA was dissolved in ethanol and n-HAp was added. After ultrasonication for 15 min, the suspensions were fed into a spray dryer (SD-06 Labplant, Labplant UK Limited, North Yorkshire, Britain) at a rate of 8 ml/min. The inlet and outlet temperatures of the drying chamber were maintained at 100°C and 50°C, respectively. The resultant powders were dried in a desiccator with a blue silica gel under reduced pressure for 1 day prior to assessment of their properties. The physical materials (PMs) were prepared by blending the components in a mortar.

In vitro dissolution study

HPLC analysis of TSIIA

The concentration of TSIIA in the dissolution medium was determined using the high-performance liquid chromatography (HPLC). The HPLC equipment included a high-performance 1200 system (Agilent technologies, CA, USA) fitted with quaternary pumps, an autosampler, a UV detector set to a wavelength of 270 nm, and a column compartment at 30°C. The HPLC stationary phase consisted of a reverse phase Agilent Zorba SB-C18 column (150 × 4.6 mm, 5 μm; Agilent Technologies Co. Ltd., USA). The mobile phase consisted of methanol and water (85:15, v: v) and was pumped isocratically at a flow rate of 1 ml/min. The samples (10 μL) were injected into the HPLC system for analysis.

In vitro dissolution studies

Dissolution studies of the samples were performed using an intellective dissolution apparatus (RCZ-8A dissolution apparatus, Precision Instruments, Tianjin University) in 900 mL of distilled water containing 0.5% sodium dodecyl sulfate at 37 ± 0.5°C. A paddle method was used at a rotation speed of 50 rpm according to ChP 10 method 2 (paddle method). The samples equivalent to 5 mg TSIIA were spread onto the surface of the dissolution medium, and 5 mL of the samples was withdrawn at 15, 30, 45, 60, 90, and 120 min. Equal volumes of fresh medium were added into the dissolution vessel after each sample was obtained. The aliquots were filtered through a 0.45-μm filter membrane, and the initial sample volume (2 ml) was discarded, resulting in a final volume of 3 ml that was collected and analyzed by HPLC. These dissolution experiments were performed in triplicate, and the average dissolution profiles and standard deviations were calculated.

DSC

DSC measurements were performed using a TA-2910-modulated calorimeter (TA Instruments, New Castle, DE, USA). Specific heat measurement was standardized using a sapphire. TSIIA, PMs, and SDs were ground for 2 min by using a mortar and pestle, and then slightly compressed in an aluminum pan by using a steel plunger. The samples (2-4 mg) were heated (25-500°C) at a constant scanning speed (5°C/min) by using nitrogen as the purging gas (50 ml/min).

SEM

SEM images of either TSIIA alone or the SD preparations were obtained using a scanning electron microscope (S-3000 N, Hitachi, Japan) with 30 kV accelerating voltage.

XRPDn-HAp

XRPD measurements of the samples were performed using an X-ray diffractometer (D8-Advance; Bruker, Karlsruhe, Germany) with a Kb filter, Cu radiation, a voltage of 25 kV, and a current of 30 mA. The powder samples were placed in a sample-holder groove and were tightly packed. They were continuously spun and scanned at a rate of 1°min^{-1} over a 2θ range of 5-70°.

FTIR

FTIR spectra of TSIIA, n-HAp, PMs, and SDs were recorded with an FTIR instrument (8400 S, Shimadzu, Japan) using KBr disk method (0.5% [w/w] of the sample). The instrument was operated under a dry air purge. The scanning range was 4000-400 cm^{-1}, and the resolution was 1 cm^{-1}.

Stability test

SDs were packed in aluminum foil and monitored for up to 6 months at a consistent ambient temperature and relative humidity (40°C/75% RH). The samples were then removed and analyzed for (1) drug content, and (2) the extent of dissolution.

RESULTS AND DISCUSSION

In vitro dissolution study

The dissolution profiles of TSIIA, PMs, and SDs at various drug-carrier ratios are shown in Figure 1. The SDs improved the dissolution rates of TSIIA to the greatest extent, unlike those observed in the case of either pure TSIIA or PMs. TSIIA exhibited a poor dissolution rate with less than 30% of the drug dissolved after 120 min. As expected, the PMs did not influence the dissolution of crystalline TSIIA. In contrast, all of the SDs prepared with the n-HAp displayed markedly improved TSIIA dissolution rates. The dissolution rate of TSIIA increased with increasing n-HAp content in the SDs. At a TSIIA: N-HAp ratio of 1:6, more than 90% of TSIIA was dissolved within 45 min, which was approximately a 6.8-fold increase compared to pure TSIIA. The SDs prepared at a TSIIA: n-HAp ratio of 1:8 showed the highest dissolution rate, with approximately 96% dissolution at 45 min. This marked improvement in the dissolution rate of TSIIA from the SDs may be explained by the reduction in particle size during the formation of the SDs, reduction of aggregation phenomena among the drug particles, and/or an increase in the effective surface area owing to more intimate particle contact and fine dispersion into the carrier.[34] Another factor that might have contributed to the increase in the dissolution rate is the rapid desorption of the drug from the n-HAp surface as previously described for silica-based excipients in the early 1970s.[35] Moreover, loss of drug crystallinity due to its nearly complete amorphous dispersion in SDs (as confirmed by DSC and XRPD studies) further supports the interpretation that the dissolution properties are enhanced by SD formulation.

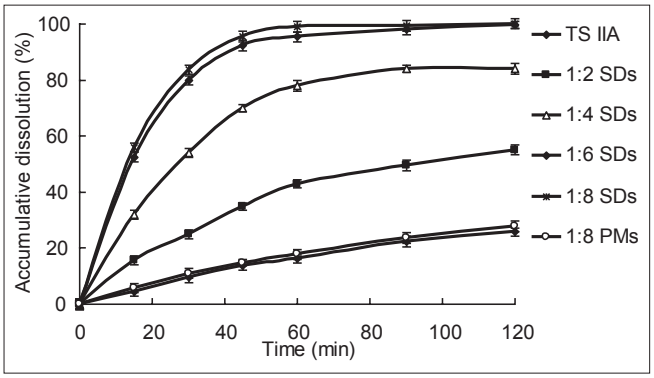

Figure 1: The dissolution profiles of Tanshinone IIA solid dispersions at different Tanshinone IIA/n-HAp ratios of 1:2, 1:4, 1:6, 1:8, and the 1:8 physical materials. Each point represents the mean ± SD value (*n*=3)

SEM

Images obtained using the SEM is shown in Figure 2. Differences between the crystalline forms can be clearly seen. An SEM image of TSIIA is shown in Figure 2a. The morphology of TSIIA was marked by irregularly shaped crystals. However, the original morphology of TSIIA was entirely altered when formulated as SDs as shown in the SEM micrographs in Figure 2b, suggesting that TSIIA homogeneously dispersed into the n-HAp carrier and thus, may exist in an amorphous form.

DSC

DSC thermograms of TSIIA, n-HAp, PMs, and SDs are shown in Figure 3. Pure TSIIA [Figure 3a] exhibited a sharp melting peak with the onset temperature of 218.9°C, indicating its crystalline nature. Similar observations have been reported by Zhao *et al*.[36] During the scanning of PMs [Figure 3c], melting and an exothermic peak of TSIIA was observed. Because a large amount of n-HAp acts as an impurity, most of the drug exists in an eutectic form. In the SDs [Figure 3d], the characteristic peak of TSIIA disappeared entirely, demonstrating that the drug may be present in the SDs in an amorphous state.

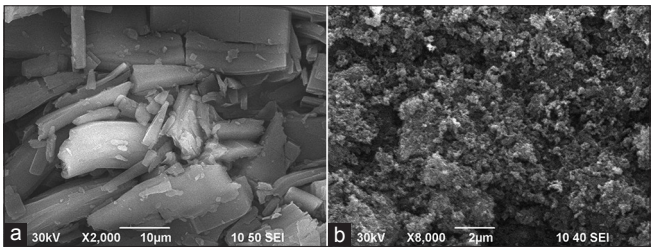

Figure 2: Photomicrographs obtained on performing scanning electron microscopy of Tanshinone IIA (a) and 1:8 (w/w) solid dispersions (b)

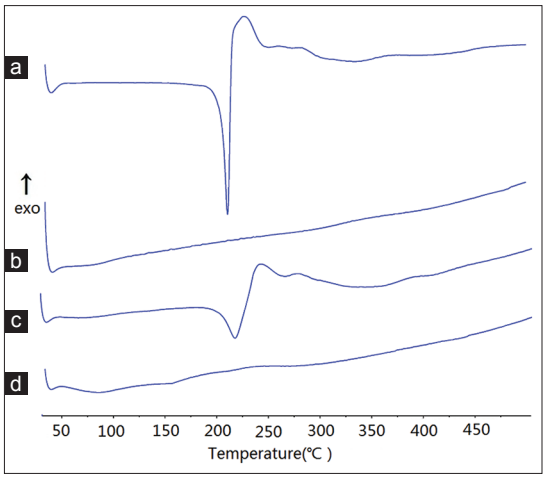

Figure 3: Differential scanning calorimetry curves of Tanshinont (a), nano-hydroxyapatite (b), 1:8 (w/w) physical materials (c), and 1:8 (w/w) solid dispersions (d)

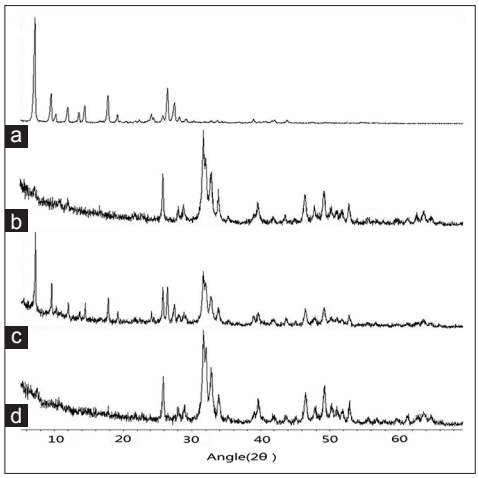

Figure 4: The X-ray powder diffractograms: Tanshinone IIA (a), n-nano-hydroxyapatite (b), 1:8 (w/w) physical materials (c), and 1:8 (w/w) solid dispersions (d)

XRPD

The crystallinity of TSIIA in PMs and SDs was examined by performing XRPD. X-ray diffraction results of TSIIA, n-HAp, PMs, and the corresponding SDs are shown in Figure 4. TSIIA [Figure 4a] showed sharp and intense peaks in the range of 5-45° 2θ, indicating its crystalline nature; n-HAp [Figure 4b] had several salient peaks between 24° and 64° 2θ. In the PM [Figure 4c], the characteristic diffraction peaks of both the carrier and the drug were present as if the sum of the components had been analyzed separately, and this pattern suggested that TSIIA existed as a crystalline form in this PM. However, in the case of the SDs, the main characteristic crystalline peaks of TSIIA were not observed, suggesting a change in the drug from a crystalline to an amorphous form [Figure 4d]. This observation was consistent with the findings of the DSC study.

FTIR

The potential interactions between TSIIA and n-HAp in the SDs were evaluated by FTIR. The spectra of TSIIA, n-HAp, PMs, and the corresponding SDs are shown in Figure 5. When scanned between 4000 nm and 400 nm, TSIIA [Figure 5a] showed characteristic carbonyl-stretching vibration absorption peaks at 1675 cm^{-1}. In this case, any sign of an interaction would reflect a change in the carbonyl vibrations and would be depend on the extent of the interaction. The spectrum of n-HAp [Figure 5b] presented characteristic signals at 1093, 1034, 602, 572, and 3570 cm^{-1} that were attributed to stretching vibrations of phosphate and OH groups.[37,38] The spectra of PMs [Figure 5c] were identical to the additive spectrum of TSIIA and n-HAp, thus indicating the absence of an interaction between TSIIA and n-HAp. However, the SDs [Figure 5d] showed an almost complete disappearance of the OH peaks at 3570 cm^{-1}, and changes were also observed in the carbonyl group. The peak at 1675 cm^{-1} shifted to 1663 cm^{-1}, probably as a consequence of hydrogen bonding between n-HAp and TSIIA during a spray drying. Hydrogen bonding played a role in maintaining the drug's stability during storage.[39]

Stability test

The lack of stability of SDs is the main problem and the primary reason for the relatively few marketed products based on SDs, despite numerous studies demonstrating their potential advantages.[40,41] Amorphous drugs formulated as SDs have a tendency to recrystallize during long-term storage, eventually resulting in impaired dissolution profiles. Temperature and humidity during storage have been reported to influence the stability of the amorphous forms of drugs. In the present study, storage conditions at ambient temperature and RH (40°C/75% RH) were adopted. SDs were stored for up to 6 months and were subjected to dissolution and drug content testing thereafter. The results of the stability test are shown in Table 1, demonstrating that the content of TSIIA remained constant during the test period. The dissolution (45 min) of TSIIA from SDs after 6 months was similar to those of SDs at day 0. These results indicate that the amorphous state of TSIIA in SDs remained nearly unchanged for 6 months. They also clearly demonstrate that n-HAp exhibited good physical stability when used for TSIIA SD formulation.

n-HAp is considered to be one of the most biocompatible and bioactive materials and has been widely accepted in medicine and dentistry in recent years.[42,43] This product consists of primary particles of approximately 60 nm in size, resulting in a relatively large surface area and enabling the production of powders on which TSIIA may be highly dispersed and/or adsorbed. The improved stability of SDs may be attributed to the adsorption of TSIIA onto the n-HAp surface, and by the interaction between TSIIA and its carrier particles,[44] as evidenced by their

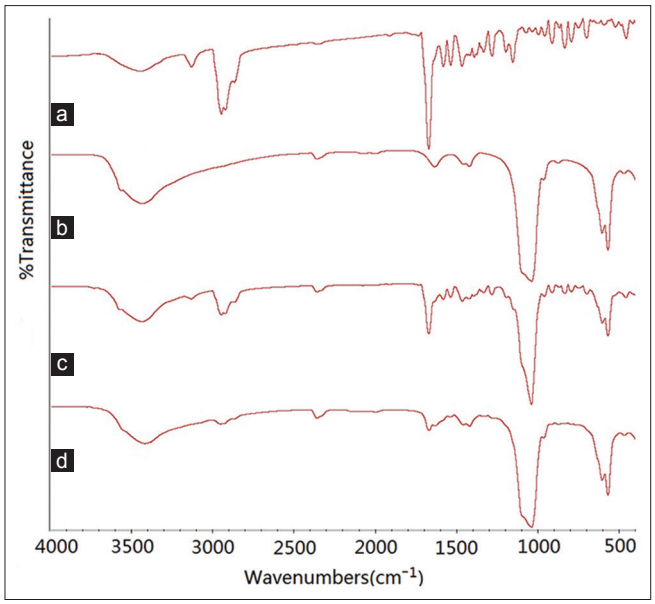

Figure 5: Spectrums obtained using infrared spectroscopy. Tanshinone IIA (a), n-nano-hydroxyapatite (b), 1:8 (w/w) physical materials (c), and 1:8 (w/w) solid dispersions (d)

Table 1: Stability test of the Tanshinone IIA solid dispersions (*n*=6, $\bar{x}$±s)

Samples	0 months		6 months	
	Drug content/ %	(45 min) dissolution rate/%	Drug content/ %	(45 min) dissolution rate/%
1:8 SDs	11.03±0.12	95.62±0.86	10.87±0.26	93.85±0.73

SDs: Solid dispersions

FTIR spectra [Figure 5]. As reported by Yang *et al*.[45] the interactions between drug and carrier particles increase the energy barrier for nucleation and the initial event of recrystallization, consequently enhancing physical stability.

CONCLUSIONS

In this study, SDs consisting of TSIIA and n-HAp were successfully prepared to use a spray-drying method. The drug dissolution behavior of TSIIA was dramatically improved in the SD formulation. The accelerated stability experiments confirmed that drug stabilization was achieved for SDs with n-HAp as a dispersing carrier. This stabilization was due to the interactions between TSIIA and its carrier particles, as well as its adsorption on the surface of n-HAp. Thus, SD preparations with n-HAp may be a promising approach for enhancing both the dissolution and stability of TSIIA.

ACKNOWLEDGMENTS

The authors report no conflicts of interest in this work. This work was supported by the Open Fund of Key Laboratory of New Drug Delivery System of Chinese Meteria Medica (2011NDDCM01001).

REFERENCES

1. Leuner C, Dressman J. Improving drug solubility for oral delivery using solid dispersions. Eur J Pharm Biopharm 2000;50:47-60.
2. Zakir F, Sharma H, Kaur K, Malik B, Vaidya B, Goyal AK, *et al*. Nanocrystallization of poorly water soluble drugs for parenteral administration. J Biomed Nano Technol 2011;7:127-9.
3. Fahr A, Liu X. Drug delivery strategies for poorly water-soluble drugs. Expert Opin Drug Deliv 2007;4:403-16.
4. Nie S, Zhang S, Pan W, Liu Y. *In vitro* and *in vivo* studies on the complexes of glipizide with water-soluble β-cyclodextrin-epichlorohydrin polymers. Drug Dev Ind Pharm 2011;37:606-12.
5. Pandya P, Gattani S, Jain P, Khirwal L, Surana S. Co-solvent evaporation method for enhancement of solubility and dissolution rate of poorly aqueous soluble drug simvastatin: *in vitro-in vivo* evaluation. AAPS Pharm Sci Tech 2008;9:1247-52.
6. Shevchenko A, Bimbo LM, Miroshnyk I, Haarala J, Jelínková K, Syrjänen K, *et al*. A new cocrystal and salts of itraconazole: Comparison of solid-state properties, stability and dissolution behavior. Int J Pharm 2012;436:403-9.
7. Frank KJ, Rosenblatt KM, Westedt U, Hölig P, Rosenberg J, Mägerlein M, *et al*. Amorphous solid dispersion enhances permeation of poorly soluble ABT-102: True supersaturation vs. apparent solubility enhancement. Int J Pharm 2012;437:288-93.
8. Mihajlovic T, Kachrimanis K, Graovac A, Djuric Z, Ibric S. Improvement of aripiprazole solubility by complexation with (2-hydroxy) propyl-β-cyclodextrin using spray drying technique. AAPS Pharm Sci Tech 2012;13:623-31.
9. Takano R, Furumoto K, Shiraki K, Takata N, Hayashi Y, Aso Y, *et al*. Rate-limiting steps of oral absorption for poorly water-soluble drugs in dogs; prediction from a miniscale dissolution test and a physiologically-based computer simulation. Pharm Res 2008;25:2334-44.
10. Chiou WL, Riegelman S. Pharmaceutical applications of solid dispersion systems. J Pharm Sci 1971;60:1281-302.
11. Sato H, Kawabata Y, Yuminoki K, Hashimoto N, Yamauchi Y, Ogawa K, *et al*. Comparative studies on physicochemical stability of cyclosporine A-loaded amorphous solid dispersions. Int J Pharm 2012;426:302-6.
12. Mizuno M, Hirakura Y, Yamane I, Miyanishi H, Yokota S, Hattori M, *et al*. Inhibition of a solid phase reaction among excipients that accelerates drug release from a solid dispersion with aging. Int J Pharm 2005;305:37-51.
13. Planinšek O, Kovačič B, Vrečer F. Carvedilol dissolution improvement by preparation of solid dispersions with porous silica. Int J Pharm 2011;406:41-8.
14. Dhumal RS, Biradar SV, Aher S, Paradkar AR. Cefuroxime axetil solid dispersion with polyglycolized glycerides for improved stability and bioavailability. J Pharm Pharmacol 2009;61:743-51.
15. Chauhan B, Shimpi S, Paradkar A. Preparation and evaluation of glibenclamide-polyglycolized glycerides solid dispersions with silicon dioxide by spray drying technique. Eur J Pharm Sci 2005;26:219-30.
16. Tripathi A, Saravanan S, Pattnaik S, Moorthi A, Partridge NC, Selvamurugan N. Bio-composite scaffolds containing chitosan/nano-hydroxyapatite/nano-copper-zinc for bone tissue engineering. Int J Biol Macromol 2012;50:294-9.
17. Kong L, Gao Y, Cao W, Gong Y, Zhao N, Zhang X. Preparation

and characterization of nano-hydroxyapatite/chitosan composite scaffolds. J Biomed Mater Res A 2005;75:275-82.

18. Kandori K, Oda S, Fukusumi M, Morisada Y. Synthesis of positively charged calcium hydroxyapatite nano-crystals and their adsorption behavior of proteins. Colloids Surf B Biointerfaces 2009;73:140-5.
19. Wei G, Ma PX. Structure and properties of nano-hydroxyapatite/polymer composite scaffolds for bone tissue engineering. Biomaterials 2004;25:4749-57.
20. Mohsen-Nia M, Massah Bidgoli M, Behrashi M, Mohsen Nia A. Human serum protein adsorption onto synthesis nano-hydroxyapatite. Protein J 2012;31:150-7.
21. Sairam Sundaram C, Viswanathan N, Meenakshi S. Uptake of fluoride by nano-hydroxyapatite/chitosan, a bioinorganic composite. Bioresour Technol 2008;99:8226-30.
22. Swetha M, Sahithi K, Moorthi A, Saranya N, Saravanan S, Ramasamy K, *et al*. Synthesis, characterization, and antimicrobial activity of nano-hydroxyapatite-zinc for bone tissue engineering applications. J Nanosci Nanotechnol 2012;12:167-72.
23. Zhou G, Hou Y, Liu L, Liu H, Liu C, Liu J, *et al*. Preparation and characterization of NiW-nHA composite catalyst for hydrocracking. Nanoscale 2012;4:7698-703.
24. Jimbo R, Coelho PG, Bryington M, Baldassarri M, Tovar N, Currie F, *et al*. Nano hydroxyapatite-coated implants improve bone nanomechanical properties. J Dent Res 2012;91:1172-7.
25. Wang P, Wu X, Bao Y, Fang J, Zhou S, Gao J, *et al*. Tanshinone IIA prevents cardiac remodeling through attenuating NAD (P) H oxidase-derived reactive oxygen species production in hypertensive rats. Pharmazie 2011;66:517-24.
26. Sun DD, Wang HC, Wang XB, Luo Y, Jin ZX, Li ZC, *et al*. Tanshinone IIA: A new activator of human cardiac KCNQ1/KCNE1 (I (Ks)) potassium channels. Eur J Pharmacol 2008;590:317-21.
27. Gao J, Yang G, Pi R, Li R, Wang P, Zhang H, *et al*. Tanshinone IIA protects neonatal rat cardiomyocytes from adriamycin-induced apoptosis. Transl Res 2008;151:79-87.
28. Fu J, Huang H, Liu J, Pi R, Chen J, Liu P. Tanshinone IIA protects cardiac myocytes against oxidative stress-triggered damage and apoptosis. Eur J Pharmacol 2007;568:213-21.
29. Li J, Wang G, Li P, Hao H. Simultaneous determination of tanshinone IIA and cryptotanshinone in rat plasma by liquid chromatography-electrospray ionisation-mass spectrometry. J Chromatogr B Analyt Technol Biomed Life Sci 2005;826:26-30.
30. Wang L, Jiang X, Xu W, Li C. Complexation of tanshinone IIA with 2-hydroxypropyl-beta-cyclodextrin: Effect on aqueous solubility, dissolution rate, and intestinal absorption behavior in rats. Int J Pharm 2007;341:58-67.
31. Chang LC, Wu CL, Liu CW, Chuo WH, Li PC, Tsai TR. Preparation, characterization and cytotoxicity evaluation of tanshinone IIA nanoemulsions. J Biomed Nanotechnol 2011;7:558-67.
32. Yu H, Subedi RK, Nepal PR, Kim YG, Choi HK. Enhancement of solubility and dissolution rate of cryptotanshinone, tanshinone I and tanshinone IIA extracted from *Salvia miltiorrhiza*. Arch Pharm Res 2012;35:1457-64.
33. Hao H, Wang G, Cui N, Li J, Xie L, Ding Z. Identification of a novel intestinal first pass metabolic pathway: NQO1 mediated quinone reduction and subsequent glucuronidation. Curr Drug Metab 2007;8:137-49.
34. Overhoff KA, Moreno A, Miller DA, Johnston KP, Williams RO 3rd. Solid dispersions of itraconazole and enteric polymers made by ultra-rapid freezing. Int J Pharm 2007;336:122-32.
35. Monkhouse DC, Lach JL. Use of adsorbents in enhancement of drug dissolution. II. J Pharm Sci 1972;61:1435-41.
36. Zhao X, Liu X, Gan L, Zhou C, Mo J. Preparation and physicochemical characterizations of tanshinone IIA solid dispersion. Arch Pharm Res 2011;34:949-59.
37. Xiao X, Liu R, Huang Q. Preparation and characterization of nano-hydroxyapatite/polymer composite scaffolds. J Mater Sci Mater Med 2008;19:3429-35.
38. Wang X, Song G, Lou T. Fabrication and characterization of nano-composite scaffold of PLLA/silane modified hydroxyapatite. Med Eng Phys 2010;32:391-7.
39. Al-Obaidi H, Ke P, Brocchini S, Buckton G. Characterization and stability of ternary solid dispersions with PVP and PHPMA. Int J Pharm 2011;419:20-7.
40. Frank KJ, Westedt U, Rosenblatt KM, Hölig P, Rosenberg J, Mägerlein M, *et al*. The amorphous solid dispersion of the poorly soluble ABT-102 forms nano/microparticulate structures in aqueous medium: Impact on solubility. Int J Nanomedicine 2012;7:5757-68.
41. Greco S, Authelin JR, Leveder C, Segalini A. A practical method to predict physical stability of amorphous solid dispersions. Pharm Res 2012;29:2792-805.
42. Li X, Huang J, Edirisinghe M. Development of nano-hydroxyapatite coating by electrohydrodynamic atomization spraying. J Mater Sci Mater Med 2008;19:1545-51.
43. Tschoppe P, Zandim DL, Martus P, Kielbassa AM. Enamel and dentine remineralization by nano-hydroxyapatite toothpastes. J Dent 2011;39:430-7.
44. Van Eerdenbrugh B, Van Speybroeck M, Mols R, Houthoofd K, Martens JA, Froyen L, *et al*. Itraconazole/TPGS/Aerosil200 solid dispersions: Characterization, physical stability and *in vivo* performance. Eur J Pharm Sci 2009;38:270-8.
45. Yang J, Grey K, Doney J. An improved kinetics approach to describe the physical stability of amorphous solid dispersions. Int J Pharm 2010;384:24-31.

Cite this article as: Jiang Y, Zhang Z, Huang S, Lu Y, Ma T, Jia X. Enhanced dissolution and stability of Tanshinone IIA base by solid dispersion system with nano-hydroxyapatite. Phcog Mag 2014;10:332-7.

Source of Support: This work was supported by the Open Fund of Key Laboratory of New Drug Delivery System of Chinese Meteria Medica (2011NDDCM01001), **Conflict of Interest:** None declared.